J. Membrane Biol. 172, 37–45 (1999)

The Journal of
Membrane
Biology

A Component of Platypus (*Ornithorhynchus anatinus*) Venom Forms Slow-Kinetic Cation Channels

J.I. Kourie

Membrane Transport Group, Department of Chemistry, The Faculties, The Australian National University, Canberra City, ACT, 0200 Australia

Received: 26 April 1999/Revised: 19 July 1999

Abstract. The lipid bilayer technique is used to examine the biophysical properties of anion and cation channels frequently formed by platypus (*Ornithorhynchus anatinus*) venom (*Oa*V). The *Oa*V-formed anion channel in 250/50 mM KCl *cis/trans* has a maximum conductance of 857 ± 23 pS ($n = 5$) in 250/50 mM KCl *cis/trans*. The current-voltage relationship of this channel shows strong inward rectification. The channel activity undergoes time-dependent inactivation that can be removed by depolarizing voltage steps more positive than the reversal potential for chloride, E_{Cl}, (+40 mV).

The reversal potential of the *Oa*V-formed slow current activity in 250/50 mM KCl *cis/trans* is close to the potassium equilibrium potential (E_K) of −40 mV. The conductance values for the slow channel are 22.5 ± 2.6 pS and 41.38 ± 4.2 pS in 250/50 and 750/50 mM *cis/trans*, respectively. The gating kinetics of the slow ion channels are voltage-dependent. The channel open probability (P_o) is between 0.1 and 0.8 at potentials between 0 and +140 mV. The channel frequency (F_o) increases with depolarizing voltages between 0 and +140 mV, whereas mean open time (T_o) and mean closed time (T_c) decrease. Ion substitution experiments of the *cis* solution show that the channel has conductance values of 21.47 ± 2.3 and 0.53 ± 0.1 pS in 250 mM KCl and choline Cl, respectively. The amplitude of the single channel current is dependent on $[K^+]_{cis}$ and the current reversal potential (E_{rev}) responds to increases in $[K^+]_{cis}$ by shifting to more negative voltages. The increase in current amplitude as a function of increasing $[K^+]_{cis}$ can be best described by a third order polynomial fit. At +140 mV, the values of the maximal single channel conductance (γ_{max}) and the concentration for half maximal γ (K_s) are 38.6 pS and 380 mM and decline to 15.76 pS and 250 mM at 0 mV, respectively. The ion selectivity of the channel to K^+, Na^+, Cs^+ and choline$^+$ was determined in ion substitution experiments. The permeability values for $P_{K^+}:P_{Na^+}:P_{Cs^+}:P_{choline^+}$ were 1:1:0.63:0.089, respectively. On the other hand, the activity of the slow channel was eliminated (Fig. 7*B*). The slow channel was reversibly inhibited by $[TEA^+]_{trans}$ and the half-maximal inhibitory concentration (K_i) was ~48 mM.

Key words: Channel-forming peptides — Muscle relaxation — Fluid and electrolyte homeostasis — Edema — Pain — Signal transduction — Inward current

Introduction

Envenomation by platypus (*Ornithorhynchus anatinus*) venom (*Oa*V) causes severe local effects, including intense pain, hyperalgesia and plasma extravasation (edema) as well as hypotension and peripheral vasodilatation in systemically administered experimental animals [6–8, 10]. The molecular mechanisms underlying these *Oa*V-induced effects are not known. Recently, it has been shown with the use of the high-performance liquid chromatography (HPLC) technique that *Oa*V contains 19 peptide and protein fractions, including a C-type natriuretic peptide (*Oa*CNP-39) and a nerve growth factor (p12/NGF), with molecular masses between 4 and 216 kD [4, 6–8]. The *Oa*CNP-39 was shown to elevate the concentrations of cGMP in aortic myocytes and to be associated with sustained tonic relaxation of the rat uterus *in vitro* [6, 7]. On the other hand, p12/NPF was thought to be involved in the activation of an inward current in dorsal root ganglia (DRGs) neurones [4, 5]. de Plater [4, 5] proposed that this inward current could underly the pain associated with platypus envenomation. However, the nature of the single ion channel(s) under-

Correspondence to: J.I. Kourie

lying these *Oa*V-induced inward currents, or any other currents, have not been known until recently.

Using the lipid bilayer technique, it has been shown that platypus venom (*Oa*V) formed a fast cation-selective channel [14, 15]. The properties of this channel, which has been traced to the C-type natriuretic peptide (*Oa*CNP-39) component of *Oa*V, include: (i) "Bursts" in the outward currents at voltages between −20 and +140 mV. These bursts are separated by well-defined periods of channel inactivation or closure. (ii) γ_{max} and K_S values of 63.1 pS and 169 mM K^+ at +140 mV and 21.1 pS and 307 mM K^+ at 0 mV, respectively. (iii) Conductance values of 38.8 ± 4.6 and 60.7 ± 7.1 pS in 250/50 and 750/50 mM *cis/trans*, respectively. (iv) *Oa*CNP-39-formed channels which are cation-selective. The selectivity sequence and permeability ratios for monovalent cations are P_{K^+}:P_{Rb^+}:P_{Na^+}:P_{Cs^+}:P_{Li^+} 1:0.64:0.28:0.13:0.06 [14].

The aim of this study is to characterize the conductance and kinetic properties of another *Oa*V-formed cation-selective channel, i.e., a slow-kinetic channel. The data obtained in this study indicate that, in addition to the *Oa*CNP-39, there are some other peptide components of the platypus venom which are capable of forming ion channels that could play a role in the of the *Oa*V-induced effects noted above.

Materials and Methods

Solutions

Unless it is otherwise stated, the initial experimental solution for incorporating *Oa*V into the bilayers contained KCl (250 mM *cis* and 50 mM *trans*) plus 1 mM $CaCl_2$ and 10 mM HEPES (pH 7.4, adjusted with 4.8 mM KOH).

Lipid Bilayer Membranes and *Oa*V Incorporation

Bilayers were formed across a 150 μm hole in the wall of a 1 ml deltrin™ cup, using a mixture of palmitoyl-oleoyl-phosphatidylethanolamine, palmitoyl-oleoyl-phosphatidylserine and palmitoyl-oleoyl-phosphatidylcholine (5:3:2, by volume) [13, 16, 20], obtained in chloroform from Avanti Polar Lipids (Alabaster, Alabama). The lipid mixture was dried under a stream of N_2 and redissolved in *n*-decane at a final concentration of 50 mg/ml. *Oa*V was then incorporated into the lipid bilayer by addition to the *cis* chamber to a final peptide concentration of 0.1–1 μg/ml. The side of the bilayer to which the *Oa*V was added was defined as *cis*, and the other side as *trans*. The experiments were conducted at room temperature between 20 and 25°C.

Recording Single Channel Activity

The pClamp6 program (Axon Instruments Foster City, CA) was used for voltage command and acquisition of Cl^- current families with an Axopatch 200 amplifier (Axon Instruments). The current was monitored on an oscilloscope and stored on compact disc recorder (CD-R). The *cis* and *trans* chambers were connected to the amplifier head stage by Ag/AgCl electrodes in agar salt-bridges containing the solutions present in each chamber. Voltages and currents were expressed relative to the *trans* chamber. Data were filtered at 1 kHz (4-pole Bessel, −3dB) and digitized *via* a TL-1 DMA interface (Axon Instruments) at 2 kHz. The formed optimal bilayers had specific capacitance values larger than 0.42 μF/cm^2, which were lower than ~1.0 μF/cm^2 value for biological membranes, because the bilayer area includes some of the thicker film of the annulus, which has a much lower capacitance.

Data Analysis

CHANNEL 2 (developed by P.W. Gage and M. Smith, at The John Curtin School of Medical Research) an in-house analysis program was used including a C-type natriuretic peptide (*Oa*CNP-39) measure the parameters of single channel activity [3, 16, 21]. These include: (i) Mean open time, T_o (i.e., the total time that the channel was not closed and including openings to all conductance levels, divided by the number of events). (ii) Mean closed time, T_c (i.e., the total time that the channel was closed divided by the number of events). (iii) Frequency of the channel opening, F_o. (iv) The open probability, P_o (i.e., the sum of all open times as a fraction of the total time). The value of the current amplitude was obtained by measuring the distance (in pA) between two lines, one set on the maximum baseline noise of the closed level, where the current amplitude is considered 0 pA, and the other was set on the noise of the majority of distinct open events longer than 0.5 msec. The reversal potential was then corrected for the liquid junction potential by using the JPCalc software [1]. Assuming that the only permeant ions ion the system were K^+ and X^+, the substituting cation, this shift ($\Delta E_{rev} = E_{X^+} - E_{K^+}$) can be used to estimate the selectivity from the following equation: $\Delta E_{rev} = 59 \log P_x + [X^+]_{cis}/P_K + [K^+]_{cis.}$

Statistics

Unless otherwise stated, each ion channel was used as its own control and the comparison was made between biophysical parameters of the channel before and after changing the *cis* or *trans* solutions by any applied treatment. Data are reported as means ± SEM of channels.

Results

Types of Ion Channels

Inward Rectifying Currents

Several ion channels that vary in their conductance and kinetic properties were regularly observed after the exposure of lipid bilayer membranes to 0.1–1 μg *Oa*V. Figure 1 shows single channel activity of the *Oa*V-formed inward currents in 250/50 mM KCl *cis/trans*. The time course of the channel activity indicates that the channel undergoes inactivation, which can be removed by depolarizing voltage steps to more negative voltages than E_{Cl} (*data not shown*). To examine the single channel inactivation, the voltage of the bilayer lipid membrane was changed, using a two-pulse voltage protocol, stepped from 0 to +80 mV for 3.4 sec and then stepped to −40 mV for 3.4 sec (Fig. 1*A*). Sixteen episodes of inward current activation and subsequent inactivation

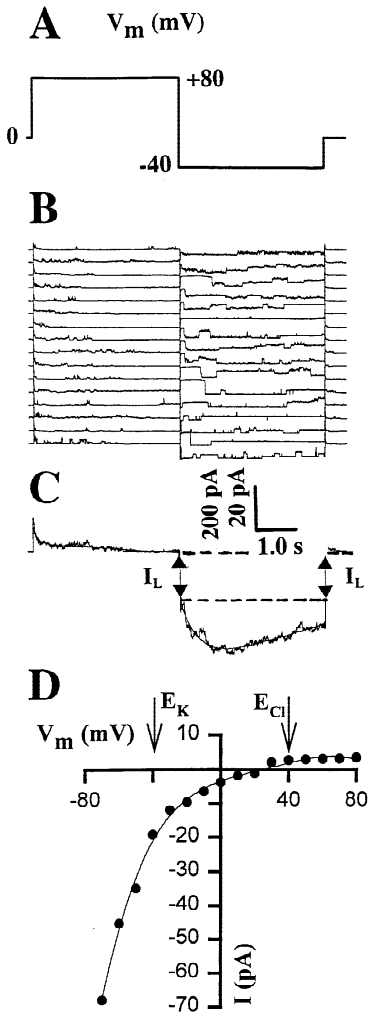

Fig. 1. Inactivation of the inwardly directed currents. (*A*) The voltage of the lipid bilayer membrane was changed, using a two-pulse voltage protocol, from 0 to +80 mV for 3.4 sec, then stepped to −40 mV for 3.4 sec. (*B*) Time course of the inward current activation and subsequent inactivation induced by the two-pulse voltage protocol for a channel in asymmetrical KCl (*cis/trans;* 250/50 mM) plus 1 mM $CaCl_2$ and 10 mM HEPES. Following convention, the downward deflections denote activation of inward currents, i.e., chloride ions moving from the *cis* chamber to the *trans* chamber. For a better display, the data are filtered at 1 kHz digitized at 2 kHz, reduced by a factor of 5, and current traces are offset by 60 pA. (*C*) The mean ensemble current through the inward-rectifying ion channel. The inactivating ensemble current is the mean of the 16 current traces shown in *B*. I_L is a constant macroscopic leak current. The solid lines are drawn to a second-order polynomial fit. The vertical scale shows 200 pA for the current traces in *B* and 20 pA for the mean ensemble current in *C*. (*D*) The current-voltage relation of the inward current for the channel activity at voltages between −80 and +70 mV. Solid line is drawn to a third-order polynomial fit. The reversal potential of the current is +27.6 mV in 250/50 mM KCl. Voltage-dependence of *Oa*V-formed ion channels.

were induced by the two-pulse voltage protocol to obtain the mean ensemble current through the inward-rectifying ion channel (Fig. 1*B*). The mean ensemble current also revealed channel inactivation (Fig. 1*C*). The time for the half change (50% decay) in the amplitude of the ensemble inward current (228 ± 24 pA; $n = 3$), calculated after subtraction of the macroscopic leak current, was 3.29 + 0.34 sec ($n = 3$) at −40 mV.

The current-voltage relationship that was constructed to examine the voltage-dependence of the *Oa*V-formed ion channel conductance exhibited strong inward rectification (Fig. 1*D*). The maximal channel conductance was 857 ± 23 pS ($n = 5$) in 250/50 mM KCl *cis/trans*. The value of the reversal potential E_{rev}, after correction for the junction potential [1], was +27.6 ± 5 mV ($n = 5$) reasonably close to the calculated Nernst (equilibrium) potential for Cl^-, E_{Cl}, (+40 mV). These findings indicate that under these experimental conditions the inward current was primarily due to the movement of Cl^- through the channel.

Outward Currents

A voltage protocol was used to examine the activity and voltage-dependency of the biophysical parameters of single channel currents in 750/50 mM KCl *cis/trans*, respectively. From an initial holding potential of 0 mV the membrane potential (V_m) was stepped to voltages ranging from −160 to +140 mV, in steps of +20 mV, for periods lasting 7 sec. The most frequently observed *Oa*V-formed outwardly directed single ion channels were those of (i) a channel with slow current kinetics (I_s), and (ii) a channel with fast or "burstlike" kinetics (I_f) (*see* 14, 15 and Fig. 2*A* and *B*). Because of the high probability of the slow channel being in the open state, the current transitions of the fast channel was generally (16 out 19) superimposed on the open state current of the slow channel in bilayers which contained both channel types (Figs. 2*A* and *B; see also* Fig. 7*A*). A significant number of bilayers contained either the slow or the fast channels. The current-voltage relationship of the slow channel exhibited weak outward rectification with a maximal slope conductance of 41.38 ± 4.2 pS ($n = 3$) in 750/50 mM KCl *cis/trans*. The current reversal potentials (E_{rev}) after correction for the junction potential [1], was more negative than −69.38 (E_K) for the slow ion channel. The only ion in the *cis* and *trans* solutions (KCl) that had a reversal potential more negative than −69.38 mV was K^+. The identification of the channel as a transporter of K^+ is therefore established by several findings: (i) its reversal potential; (ii) shift in the reversal potential upon changing $[K]_{cis}$; (iii) ionic composition of the bath, i.e., K^+ is the main cation in the solution (*see below*); (iv) monovalent ion substitution experiments; (v) block with TEA^+ a K^+ channel blocker (*see below*). These findings together indicate that the outward currents were primarily due to the movement of K^+ from the *cis* to the *trans* chamber. The remainder of this paper is confined to examining the properties of this slow cation channel.

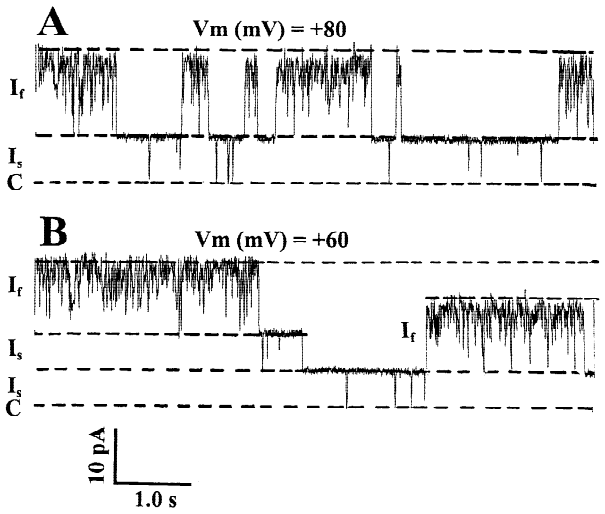

Fig. 2. Representative *Oa*V-formed single ion channels. Current traces illustrating the activity of slow (I_s) and fast (I_f) cation channels recorded at (*A*) +80 mV and (*B*) +60 mV in asymmetrical KCl (*cis/trans;* 750/50 mM) plus 1 mM $CaCl_2$ and 10 mM HEPES. Following convention, the upward deflections from the closed level, *C*, denote activation of outward cation current, i.e., potassium ions moving from the *cis* chamber to the *trans* chamber. For a better display, the data are filtered at 1 kHZ, digitized at 2 kHz and reduced by a factor of 11. Note the activation of one slow and one fast channel at +80 mV. Note also the activation of one fast and two slow channels at +60 mV; after 3.8 sec, one of the slow channels is inactivated.

Potassium-Dependency of the Slow Ion Channel

The cationic nature of the channel was determined in ion substitution experiments (Fig. 3). The *cis* solution containing 250 mM KCl was totally replaced by another solution containing 250 mM choline Cl (Fig. 3*A* and *B*). This eliminated the channel activity and reduced the unitary channel conductance from 21.47 ± 2.3 pS ($n = 3$) to 0.53 ± 0.1 pS ($n = 3$) at +140 mV. The current reversal potentials (E_{rev}) shifted from −29.5 ± 4.8 mV in 250 mM KCl to +31.8 ± 3.2 mV in 250 mM choline Cl (in addition to the 4.8 mM KOH used to buffer the pH to 7.4). These findings taken together further support the suggestion that the movement of K^+ underlies the outward currents.

The dependence of the current-voltage relation of the outward current on $[K^+]_{cis}$ was examined at concentrations between 250 and 750 mM and families of current traces were obtained. The constructed current-voltage relationships show weak outward rectification and increases in current amplitude (Fig. 4*A*). E_{rev}, as expected, responded to changes in $[K^+]_{cis}$ by shifting to negative values from −22 to −39, −50, −78, −87 and −87 mV at 250, 350, 450, 550, 650 and 750 mM $[KCl]_{cis}$, respectively. It should be noted that the apparent discrepancy between E_{rev} and E_K for 650 and 750 mM KCl disappears if these are estimated from a third-order exponential fit. However, for consistency with other $[KCl]_{cis}$ they are drawn to a second-order exponential fit.

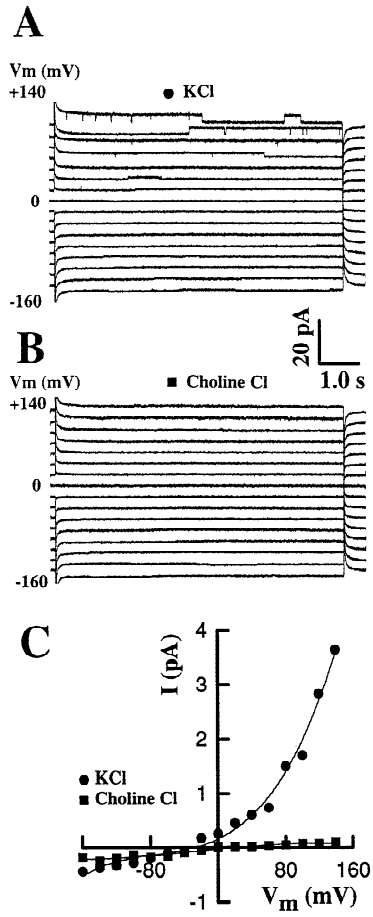

Fig. 3. The cationic nature of the *Oa*V-formed slow cation channel. Single channel currents activated at different voltages between −160 and +140 mV in: (*A*) (●) 250/50 mM KCl and (*B*) (■) same channel after substitution of 250 mM $[KCl]_{cis}$ with 250 mM $[choline\ chloride]_{cis}$. (*C*) Current voltage-relationships in (●) 250/50 mM KCl and (■) 250/50 mM choline chloride. The solid lines are drawn to a second-order polynomial.

The increase in the current amplitude as a function of increasing $[K^+]_{cis}$ was nonlinear (Fig. 4*B*), indicating that K^+ binds to sites in the channel pore. The outward current was best described by a third order polynomial fit. At +140 mV, the values of the maximal single channel conductance (γ_{max}) and the concentration for half maximal γ (K_S) are 38.6 pS and 380 mM and decline to 15.76 pS and 250 mM at 0 mV, respectively. It is suggested that current saturation resulted from a binding and unbinding step of K^+ to the channel protein; this step limits the permeation of K^+ through the channel at high ionic concentrations [12]. The values of γ_{max} and K_S decline to 15.76 pS and 250 mM at 0 mV, respectively.

Ion Selectivity of the Slow Channel

The ion selectivity of the channel to K^+, Na^+ and Cs^+ was determined in ion substitution experiments. The 250 mM

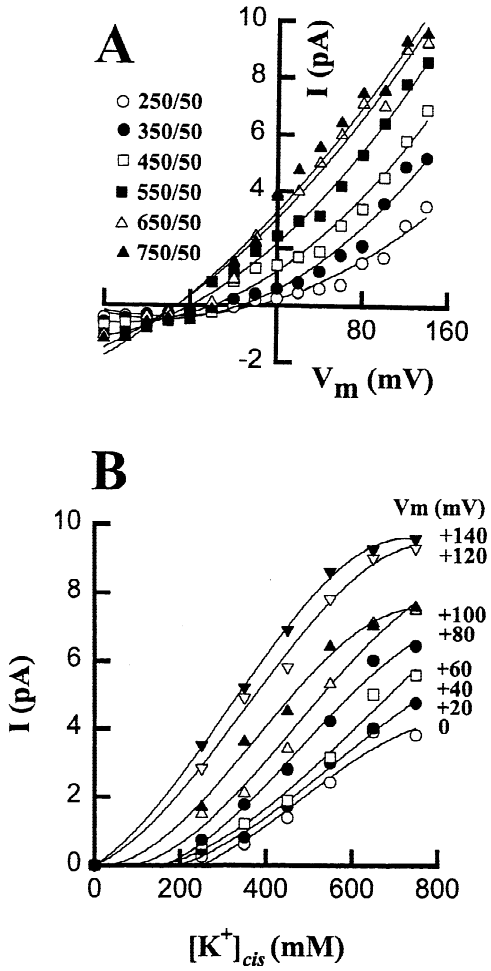

Fig. 4. Dependency of the *Oa*V-formed slow channel on $[KCl]_{cis}$. (*A*) Current voltage-relationships at 250 (○), 350 (●), 450 (□), 550 (■), 650 (△), and 750 mM $[KCl]_{cis}$ (▲). The solid lines are drawn to a second-order exponential fit. Using these fits to estimate E_{rev}, the values were −22, −39, −50, −78, −87 and −87 mV at 250, 350, 450, 550, 650 and 750 mM $[KCl]_{cis}$, respectively. It should be noted that the apparent discrepancy between E_{rev} and E_K for 650 and 750 mM KCl disappears if these are estimated from a third-order exponential fit. However, for consistency with other $[KCl]_{cis}$ they are drawn to a second-order exponential fit. (*B*) Michaelis-Menten curves for the single channel current amplitude as a function of $[KCl]_{cis}$ at different voltages between 0 (bottom) and +140 mV (top) in +20 mV steps. 0 (○), +20 (●), +40 (□), +60 (■), +80 (△), +100 (▲), (+120 (▽), and +140 mV (▼). The solid lines are drawn to a third-order polynomial.

KCl in the *cis* chamber was totally replaced by 250 mM of either NaCl or CsCl, and families of current traces were obtained at voltages between −160 and +140 mV (Fig. 5*A*). The constructed current-voltage relationships from these current families reveal no significant reduction in the current amplitude or shift in the E_{rev} of the channel in a solution containing 250 mM NaCl (Fig. 5*B*). However, the current amplitude was reduced and E_{rev} shifted by +10 mV in the presence of 250 mM CsCl (Fig. 5*C*). The reversal potential in 250/50 mM (*cis/trans*) KCl or NaCl was −38 and −30 mV in 250/50 mM (*cis/trans*) CsCl (Fig. 5*D*). The calculated permeability values obtained from conductance and zero-current potentials under bi-ionic conditions (Figs. 3 and 5) for $P_{K^+}:P_{Na^+}:P_{Cs^+}:P_{choline^+}$ were 1:1:0.63:0.089, respectively. Different phospholipid compositions, e.g., PE:PS = 70:30, PE:PS:PC = 50:30:20 PE:PC 80:20 and PE:PC 50:50 were also used to form bilayers. Ion channel proteins/peptides incorporated into bilayers with neutral and negative net charges produced similar ion channel activity. This rules out cation selectivity for the channel as a result of a PS-induced Gouy-Boltzmann (Chapman) effect [*see* ref. 11]. In addition, not all peptides incorporated into net negative bilayers form cation selective channels [16].

Kinetics of Single Channels

The kinetic parameters of the *Oa*V-formed slow channels were obtained by analyzing channel activity recorded at positive voltages (Fig. 6). The voltage-dependent kinetic-parameters, P_o and F_o, increased while T_o and T_c decreased as the bilayer was made more positive between 0 and +140 mV (Fig. 6*A–D*). The channel open probability (P_o) was between 0.1 and 0.8 at potentials between 0 and +140 mV. The channel gating parameters were independent of $[KCl]_{cis}$ ranging between 50 and 750 mM (*data not shown*). On the other hand, the replacement of the 250 mM KCl in the *cis* chamber by 250 CsCl increased F_o and reduced T_o and T_c (Fig. 6*B–D*), whereas P_o did not appear to be affected significantly (Fig. 6*A*).

Pharmacology of the *Oa*V-Formed Slow Ion Channels

The slow and fast channels differ in their sensitivity to TEA^+. Figure 7 shows current activity recorded at +150 and +160 mV, in both the absence and presence of TEA^+ in the *trans* solutions, from a bilayer that contained one fast and one slow channel. It is apparent that the unitary current of the fast channel was not affected even by 100 mM $[TEA^+]_{trans}$ (a blocker of the outwardly rectifing K^+ channel) (Fig. 7*A*), being ~8.46 pA at +160 mV in both the absence and the presence of TEA^+. On the other hand, the activity of the slow channel was eliminated (Fig. 7*B*). The dependence of the slow channel on $[TEA^+]_{trans}$ was examined between 0 and 100 mM. The current amplitude, *I*, was decreased by 10–20% at 20 mM $[TEA^+]_{trans}$ and 90–100% at 80 mM. The current inhibition was fully reversible after wash with control *trans* solution. The current amplitude at different $[TEA^+]_{trans}$, $I_{[TEA^+]trans}$ expressed relative to the current amplitude for

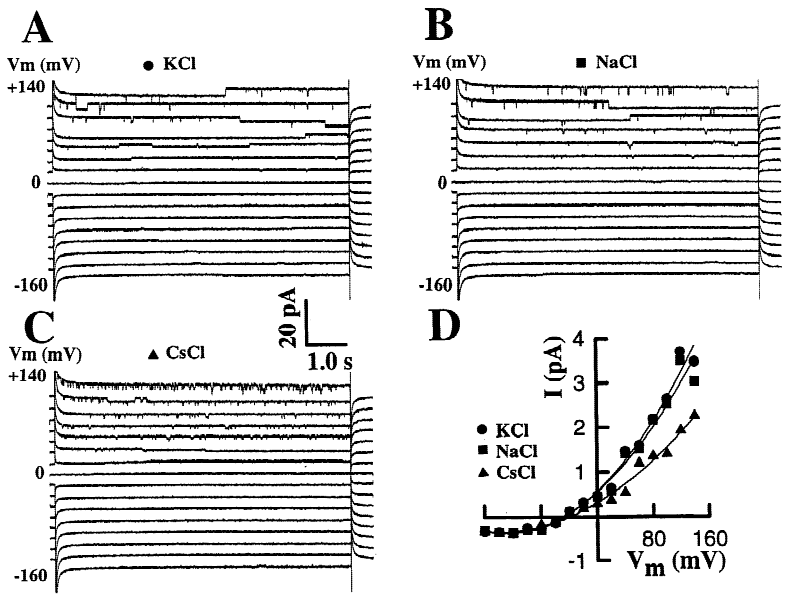

Fig. 5. Ion selectivity of the *Oa*V-formed slow ion channel. Single channel currents activated at different voltage and in: (*A*) 250 mM $[KCl]_{cis}$, (*B*) 250 mM $[NaCl]_{cis}$, and (*C*) 250 mM $[CsCl]_{cis}$. (*D*) Current voltage-relationships for different cations: (●) K^+, (■) Na^+, and (▲) Cs^+.

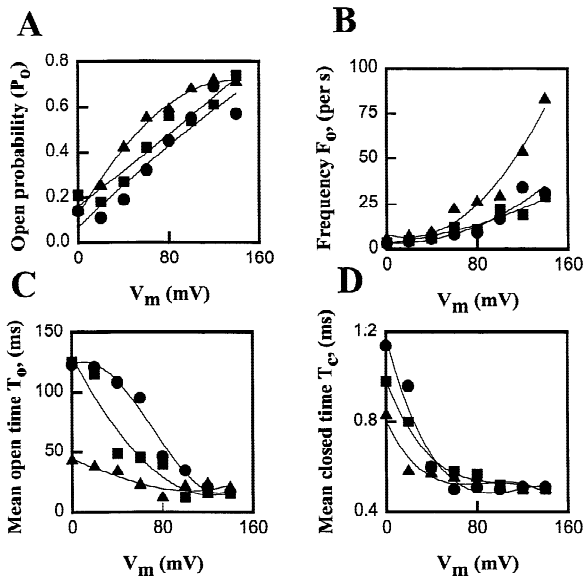

Fig. 6. Voltage-dependence of the kinetic parameters of the *Oa*V-formed slow channel. (*A*) Open probability (P_o) (*B*) frequency F_o, (*C*) mean open time T_o and (*D*) mean closed time T_c. The threshold for channel detection was set at 50% of the current amplitude and *cis* solution of 250 mM (●) KCl, (■) NaCl and (▲) CsCl. The solid lines are drawn to a second-order polynomial fit in (*A* and *B*) and to a third-order polynomial fit in (*C* and *D*). The data are means of two to three channels.

control, $I_{control}$, is shown in Fig. 8. The half-maximal inhibitory concentration (K_i) of $[TEA^+]_{trans}$ was ~48 mM.

Discussion

The Protein/Peptide Origins of The *Oa*V-Formed Ion Channels

The lipid bilayer technique is a powerful tool for characterizing single ion channel properties. Until now, there have been no reports of *Oa*V-formed ion channels but the data reported here show several types of novel *Oa*V-formed ion channels. These channels vary in their selectivity, conductance, kinetics and voltage-dependent properties. The ion channels observed in artificial lipid bilayer membranes originate from different protein and peptide components of the platypus venom. The lipid bilayer technique can provide an important analytical assay for the purification of *Oa*V components underlying different ion channel types. Unfortunately, the isolation and purification of the *Oa*V protein components is hindered by the limited supplies of this venom from the platypus, which is an endangered species in Australia. Currently, neither the component of the *Oa*V which forms the slow outward-directed cation channel nor the molecular mechanism of the protein/peptide incorporation into the bilayer are known. However, it is unlikely that this channel is due to either (i) the *Oa*CNP-39 component in the *Oa*V that forms the ~60 pS fast channel (14) or (ii) p12/NGF, which induces inward currents [4]. It should be noted that the p12/NGF-inward currents could be due to channel formation and/or modification of inwardly directed channels that are intrinsic to the membrane.

Characteristics of *Oa*V-Formed Slow Channels

The mean conductance of the slow ion channel in lipid bilayer membranes is 22.5 ± 2.6 pS in 250/50 mM KCl and 41.38 + 4.2 pS in 750/50 mM *cis/trans*. The current reversal potential of −40 mV in 250/50 mM KCl is closer to the E_K value than that of E_{Cl}, indicating that this channel is more selective for cations than for anions. The selectivity sequence of the slow channel, determined from the shift in the reversal potential under bi-ionic

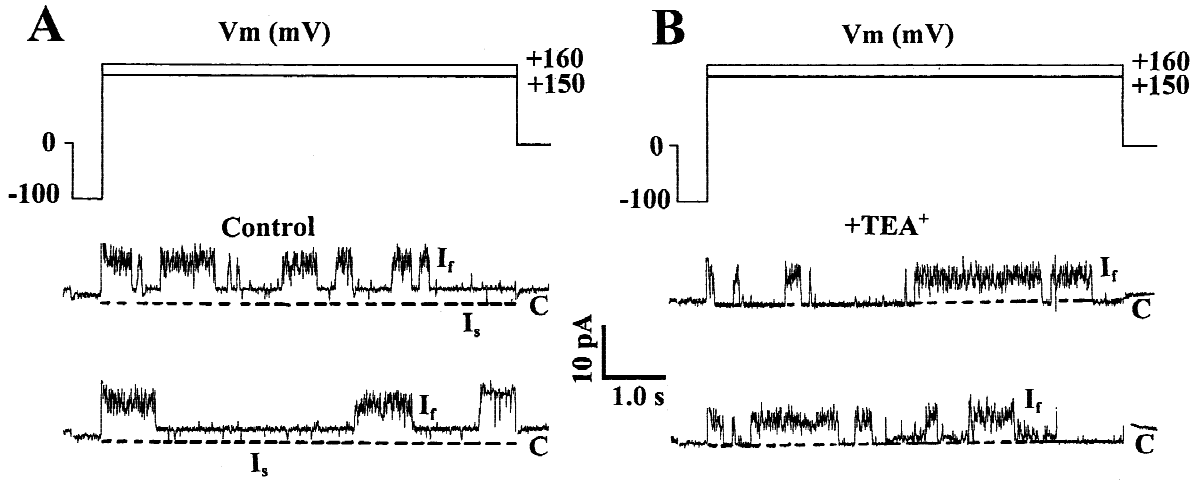

Fig. 7. *Oa*V-formed slow (I_s) and fast (I_f) channels, recorded from a bilayer in 250/50 mM KCl. (*A*) Control, and (*B*) 100 mM $[TEA^+]_{trans}$. Shown above the current traces in *A* and *B* are voltage steps used to induce single channel currents. The current races for the control shown in (*A*) reveal the presence of both the fast and the slow channels. The addition of TEA^+ blocks the slow channel without affecting the fast channel (*B*). The broken lines in (*A*) denote the closed state, '*C*', for the slow channel.

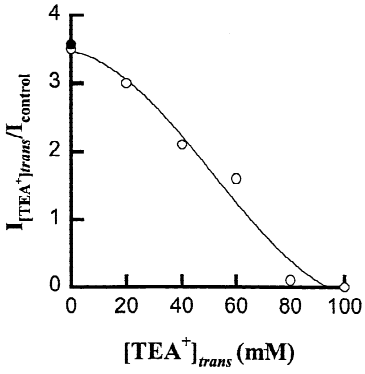

Fig. 8. Dose-dependent effects of milimolar TEA^+ added to *trans* solution ($[TEA^+]_{trans}$) on relative current of slow cation-selective channel. $I_{[TEA^+]_{trans}}$ is given for different $[TEA^+]_{trans}$ relative to control (no TEA^+). The solid line is drawn to a third-order polynomial fit of the data (○). The effect of $[TEA^+]_{trans}$ was reversible after wash with control *trans* solution (●).

solutions and conductance measurements in 250 mM cation chloride, was in the order $K^+ > Na^+ > Cs^+$, which could agree with either of Eisenman sequences V and VI [12]. The most distinctive feature of the slow channels is the low frequency of current transition between the open and the closed states. However, like most outward K^+ currents, the slow channel was inhibited by rather high concentrations of TEA^+ (K_i = ~48 mM) on the luminal side of the membrane. In contrast to the inward current, the time course of the outward currents did not appear to indicate channel inactivation. Neither the regulatory mechanisms nor the extent of the channel opening are known for this channel *in vivo*. The voltage regulation of channel kinetics does not rule out other regulatory mechanisms.

Other Toxin-Formed Ion Channels and the Pathophysiological Significance of *Oa*V-Formed Channels

The conductance and kinetics of the *Oa*V-formed cation channels differ from the previously described peptide- or toxin-formed voltage-dependent cation channels (Table). The current-voltage relations for the *Oa*V-formed fast (burstlike activity) and slow cation channels show outward rectification. The conductance values for the slow and fast channels are 22.5 ± 2.6 pS and 38.8 ± 4.6 pS in 250 mM *cis/trans* and 41.38 ± 4.2 pS and 60.7 ± 7.1 pS in 750/50 mM *cis/trans*. The gating kinetics of the slow ion channels were voltage-dependent. The channel open probability (P_o) is between 0.1 and 0.8 at potentials between 0 and +140 mV. The channel frequency (F_o) increased, whereas mean open time (T_o) and mean closed time (T_c) times decreased with depolarizing voltages between 0 and +140 mV. Ion substitution experiments of the *cis* solution show that the channel has conductance values of 21.47 ± 2.3 and 0.53 + 0.1 pS in 250 mM KCl and choline Cl, respectively. At +140 mV, γ_{max} and K_S values were 38.6 pS and 380 mM and declined to 15.76 pS and 250 mM at 0 mV. The permeability values for $P_{K^+}:P_{Na^+}:P_{Cs^+}:P_{choline^+}$ were 1:1:0.63:0.089, respectively.

A number of *Oa*V peptides have been implicated in *Oa*V-induced pathologies, which include intense pain, edema and persistent hyperalgesia [4]. These effects of envenomation, obviously, could arise from both the interaction with intrinsic ion transport pathways and the *Oa*V-formation of new transport pathways. Both factors would augment the abnormal electrical activity and the distortion of signal transduction, causing loss of membrane compartmentation. Our current working hypothesis is that the *Oa*V mediates its pathophysiological ef-

Table. Properties of some toxins and CNP-39-formed ion channels

Peptide type	Channel type and selectivity	Method	Concentration of *cis/trans* (mM)	Conductance (pS) *I-V* relations Blockers	Amino acid sequence and mechanism of channel formation	Pathology	Reference
Diphtheria toxin	Voltage-dependent anion selective channel P_{Cl}/P_{Na} 6	Incorporated into PE at pH 5.0–4	200 mM NaCl 1000 mM NaCl	6.2 20 Linear at positive voltages and sublinear at negative voltages	22 kDa protein aggregation	Diphtheria	(9)
Tetanus toxin (TeTx)	Voltage-dependent cation selective channel $P_K/P_{Na} \geq 1.35$	Incorporated into PS at neutral pH	500/500 KCl	89 at pH 7.0 30 at pH 30 Larger at positive voltages than at negative voltages	140 kDa N-terminal fragment 95 kDa (channel forming fragment) C-terminal fragment 50 kDa	Spasticity and convulsions (human tetanus)	(11)
Staphylococcal δ-toxin	Voltage-dependent and voltage-independent cation channels P_K/P_{Cl} 9.3 small P_K/P_{Cl} 2.6 large	0.1 to 2.0 μM Incorporated into PC bilayer pH 7.0	500/500 KCl	Small channel 70–100 Large channel 450 pS Linear around 0 mV Nonlinear voltages greater than 60 mV	Tetrameric and higher aggregates in aqueous solution MAQDIISTIG-DLVKWIID-TYMKFTKK	Adverse effects on biological membranes	(18)
Aerolysin a cytolytic protein	Voltage-dependent, slight anion selective channel P_{Cl}/P_{Na} 3.6	3–6 μg/ml Incorporated into PC bilayer pH 7.0–7.4	100 NaCl 1000 NaCl	145 420	50 kDa protein, histidine-induced oligomeric complexes and inhibited by Zn^{2+}	Destroy Osmotic lysis	(2,23)
Clostridium botulinum C2 toxin	Voltage-dependent cation-selective	PC or PS	100 KCl	55	Inhibited by chloroquine	ADP-ribosy-lating-induced destruction of the actin cycloskeleton	(22)
Hemolysin HlyA a cytolytic toxin	Voltage-dependent moderately anion selective channel P_{Cl}/P_{Na} 6.6	1–10 μM Peptide incorporated into lipid bilayer azolectin phosphotadyl-choline, GPA	100 KCl 1000 KCl	22 350	220 kDa protein, oligomeric complexes	Effects via cAMP-stimulated Cl- and HCO^{3-} efflux from the intestinal cells (cholera)	(19)
CNP-39 A peptide component of platypus venom	Fast K^+ channel $K^+ > Rb^+ > Na^+ > Cs^+$ $Li^+ >>$ Choline	0.1–1 μg/ml PE:PS:PC 50:30:20	250/50 KCl 750/50 KCl	38.8 60.7	LLHDHPNPRK-YKPAYKKGL-SKGCFGLKL-DRIGSTSGLGC Oligomeric complexes	Vasodilation, changes in electrolyte homeostasis, kidney failure, envenomation	(14)

fects by forming ion channels which modify the membrane potential and second messenger systems, e.g., Ca^{2+} homeostasis and cGMP production [14, 17]. The *Oa*V-formed ion channels may dissipate K^+ and Cl^- gradients essential for electrolyte homeostasis and thereby resulting in the symptoms of edema. It has been suggested that the inward macroscopic current, which is produced by *Oa*V and has been linked to the p12/NGF component in dorsal root ganglia (DRGs) neurons, may underlie the long-term and severe pain associated with platypus envenomation [4, 5]. The time course of the ensemble averaged current of the single inward currents reveals inactivation similar to *Oa*V-induced inward macroscopic currents in DRGs. Whether the single inwardly rectifying anion channels (Fig. 1) in fact do underline the macroscopic currents is an issue that can only be resolved by further characterization of this current at the single channel level.

In conclusion, it is proposed that these *Oa*V-formed ion channels underlie changes in the signal transduction mechanisms, which may explain, at least partly, the reported symptoms of envenomation and the vasodilatory effects in smooth muscles [6–8].

I would like to thank Mr. R. McCart and Mr. H. Wood for numerous discussions, suggestions and critical reading of the manuscript. I also thank Dr. G.M. de Plater for his generous gift of the platypus venom. The laboratory assistance of Ms. A. Culverson, Ms. C. Horan and Ms. E. Sturgiss of the CSIRO Student Research Scheme is greatly appreciated. This research work is supported by a National Health and Medical Council project grant (number 970122).

References

1. Barry, P.H. 1994. JPCalc, a software package for calculating liquid junction potential corrections in patch-clamp, intracellular, epithelial and bilayer measurements and for correcting junction potential measurements. *J. Neurosci. Meth.* **51:**107–116
2. Buckley, J.T. 1992. Crossing three membranes. Channel formation by aerolysin. *FEBS Lett.* **307:**30–33
3. Colquhoun, D., Hawkes, A.G. 1983. Fitting and statistical analysis of single-channel recording. *In:* Single Channel Recording. B. Sakmann and E. Neher. Editor pp. 135–175. Plenum, New York.
4. de Plater, G.M. 1998. Fractionation, primary structural characterization and biological activities of polypeptides from the venom of the platypus (*Ornithorhynchus anatinus*). PhD thesis. Australian National University. Canberra Australia.
5. de Plater, G.M. 1998. Platypus (*Ornithorhynchus anatinus*) venom activates a Ca^{2+}-dependent inward current in rat dorsal root ganglion neurones. *J. Physiol.* **506:**154*P*
6. de Plater, G.M., Martin, R.L., Milburn, P.J. 1995. A pharmacological and biochemical investigation of the venom from the platypus (*Ornithorhynchus anatinus*). *Toxicon* **33:**157–169
7. de Plater, G.M., Martin, R.L., Milburn, P.J. 1998. The natriuretic peptide (ovCNP) from platypus (*Ornithorhynchus anatinus*) venom relaxes the isolated rat uterus and promotes oedema and mast cell histamine release. *Toxicon* **36;**847–857.
8. de Plater, G.M., Martin, R.L., Milburn, P.J. 1998. A C-type natriuretic peptide from the venom of the platypus (*Ornithorhynchus anatinus*): structure and pharmacology. *Comp. Biochem. Physiol. C.* **120:**99–110
9. Donovan, J.J., Simon, M.I., Draper, R.K., Montal, M. 1981. Diphtheria toxin forms transmembrane channels in planar lipid bilayers. *Proc. Natl. Acad. Sci. USA* **78:**172–176
10. Fenner, P.J., Williamson, J.A., Myers, D. 1992. Platypus envenom—a painful learning experience. *Med. J. Aust.* **157:**829–832
11. Gambale, F., Montal, M. 1988. Characterization of the channel properties of tetanus toxin in planar lipid bilayers. *Biophys. J.* **53:**771–783
12. Hille, B. 1992. Ionic Channels of Excitable Membranes. 2nd ed: Sinaur Associates, Sunderland
13. Kourie, J.I. 1996. Vagaries of artificial bilayers and gating modes of the SCl channel from the sarcoplasmic reticulum of skeletal muscle. *J. Membr. Sci.* **116:**221–227
14. Kourie, J.I. 1999. Characterization of a C-type natriuretic peptide (CNP-39)-formed cation-selective channel from platypus (*Ornithorhynchus anatinus*) venom. *J. Physiol.* **518:**359–369
15. Kourie, J.I. 1999. Calcium-dependence of C-type natriuretic peptide-formed fast K^+ channel. *Am. J. Physiol.* (*in press*)
16. Kourie, J.I., Laver, D.R., Junankar, P.R., Gage, P.W., Dulhunty, A.F. 1996. Characteristics of two types of chloride channel in sarcoplasmic reticulum vesicles from rabbit skeletal muscle. *Biophys. J.* **70:**202–221
17. Kourie, J.I., Rive, M.J. 1999. Role of natriuretic peptides in ion transport mechanisms. *Medici. Res. Rev.* **19:**75–94
18. Mellor, I.R., Thomas, D.H., Sansom, M.S. 1988. Properties of ion channels formed by *Staphylococcus aureus* delta-toxin. *Biochim. Biophys. Acta* **942:**280–294
19. Menzl, K., Maier, E., Chakraborty, T., Benz, R. 1996. HlyA hemolysin of *Vibrio cholerae* 01 biotype El Tor—identification of the hemolytic complex and evidence for the formation of anion-selective ion-permeable channels. *Eur. J. Biochem.* **240:**646–654
20. Miller, C., Racker, E. 1976. Ca^{++}-induced fusion of fragmented sarcoplasmic reticulum with artificial planar bilayers. *J. Membrane Biol.* **30:**283–300
21. Patlak, J.B. 1993. Measuring kinetics of complex single ion channel data using mean-variance histograms. *Biophys. J.* **65:**29–42
22. Schmid, A., Benz, R., Just, I., Aktories, K. 1994. Interaction of *Clostridium botulinum* C2 toxin with lipid bilayer membranes. Formation of cation-selective channels and inhibition of channel function by chloroquine. *J. Biol. Chem.* **269:**16706–16711
23. Wilmsen, H.U., Pattus, F., Buckley, J.T. 1990. Aerolysin, a hemolysin from *Aeromonas hydrophila*, forms voltage-gated channels in planar lipid bilayers. *J. Membrane Biol.* **115:**71–81